EUROPEAN ORGANIZATION FOR NUCLEAR RESEARCH
European Laboratory for Particle Physics

LHC Hadron Collider **LHC Project Report 74**

Boundary-Induced Coupling Currents in a 1.3 m Rutherford-type Cable due to a Locally Applied Field Change

A.P. Verweij
CERN, CH1211 Geneva 23, Switzerland
M.P. Oomen, and H.H.J. ten Kate
University of Twente, Applied Superconductivity Centre, PO Box 217, 7500 AE Enschede, The Netherlands

Abstract

In this paper the existence of so called Boundary-Induced Coupling Currents (BICCs) is experimentally demonstrated in a 1.3 m long Rutherford-type cable. These BICCs are induced by applying a field change locally onto the cable and can be represented by a non-uniform current distribution between the strands of the cable during and after the field sweep. In order to better understand the characteristic time, amplitude and characteristic length of these coupling currents and the parameters by which they are influenced, a special set-up has been built. With this set-up it is possible to scan the field induced by the BICCs along the full length of a Rutherford-type cable. Special attention is paid on the influence of the contact resistance between crossing strands on the characteristics of the BICCs, and results are presented where parts of the cable are soldered, simulating the joints of a coil.

LHC Division / * University of Twente, The Netherlands

ASC Pittsburgh ‘96

Administrative Secretariat
LHC Division
CERN
CH -1211 Geneva 23
Switzerland

Geneva, 15 November, 1996

Boundary-Induced Coupling Currents in a 1.3 m Rutherford-type Cable due to a Locally Applied Field Change

A.P. Verweij
CERN, CH1211 Geneva 23, Switzerland
M.P. Oomen, and H.H.J. ten Kate
University of Twente, Applied Superconductivity Centre, PO Box 217, 7500 AE Enschede, The Netherlands

***Abstract* - In this paper the existence of so called Boundary-Induced Coupling Currents (BICCs) is experimentally demonstrated in a 1.3 m long Rutherford-type cable. These BICCs are induced by applying a field change locally onto the cable and can be represented by a non-uniform current distribution between the strands of the cable during and after the field sweep. In order to better understand the characteristic time, amplitude and characteristic length of these coupling currents and the parameters by which they are influenced, a special set-up has been built. With this set-up it is possible to scan the field induced by the BICCs along the full length of a Rutherford-type cable. Special attention is paid on the influence of the contact resistance between crossing strands on the characteristics of the BICCs, and results are presented where parts of the cable are soldered, simulating the joints of a coil.**

I. Introduction

Recently Boundary-Induced Coupling Currents (BICCs), or often called Super (Coupling) Currents, are theoretically proved to exist in Rutherford-type cables [1]-[6]. A good understanding of BICCs is important since they cause sinusoidally varying field errors during and after a field ramp and affect the ramp-rate sensitivity and stability of coils. BICCs are mainly caused by non-uniformities along the cable length of the field change $\dot{B}_\perp$ (perpendicular to the broad cable face) and/or the contact resistance R_c between crossing strands. The effect of a field change parallel to the broad face of the cable, and the effect of a varying contact resistance between adjacent strands are small and are disregarded in this paper.

Besides a qualitative understanding of BICCs, the use of a network model [3],[4],[6] has as well resulted in a quantitative estimate of the magnitude and the characteristic time of the BICCs and the length over which the BICCs diffuse along the cable. The formulas are derived for single $\dot{B}_\perp$- and R_c-steps whereas more complex $\dot{B}_\perp$- and R_c-distributions can be dealt with by superposition of many small steps. These formulas show that (for uniform R_c):

- BICCs penetrate along the cable over an effective length which depends on the ratio between R_c and the effective resistivity ρ_{bi} which the BICCs "see" along the length (probably related to the diffusion process of the BICCs from the contacts into the filaments through the matrix). In the experiment described in this paper R_c is relatively large and the BICCs flow till both ends of the cable.
- The magnitude of the BICCs is proportional to $\dot{B}_\perp(l_{cab,1}l_{cab,2})/[(l_{cab,1}+l_{cab,2})\cdot R_c]$, with $l_{cab,1}$ and $l_{cab,2}$ the distances from the non-uniformity to the cable ends.
- The characteristic time $\tau_{bi}(z)$ of the BICCs at position z, taken as the period during which the field B_{bi} at position z has decayed to 1/e of its steady-state value, is linear to $(l_{cab,1}l_{cab,2})/R_c$. Time τ_{bi} increases in first order linearly along the length and is minimum at the $\dot{B}_\perp$ non-uniformity.

The major problem in estimating the BICCs in a coil is related to the unknown ρ_{bi} and to interaction of the BICCs produced by the numerous non-uniformities. The characterisation of BICCs in magnets, by means of measurements of the magnetic field in the aperture of a magnet [7],[8] can therefore hardly be used to validate these formulas quantitatively.

In order to prove the existence of BICCs and to validate the formulas, a new experimental set-up has been designed and constructed. It is based upon the measurement of the magnetic field, caused by the BICCs, along the length of a single straight cable.

The cable can be locally subjected to a $\dot{B}_\perp$-variation and R_c can be spatially changed. A description of the set-up and the features that can be implemented are given in section II.

A discussion of the experimental results and a comparison with numerical calculations is given in section III.

II. Experimental Setup

The schematic front view and cross-section are shown in Fig. 1. The set-up is installed vertically in a cryostat, operating at 4.2 K. A 17 mm wide keystoned Rutherford-type cable (having 26 strands with SnAg coating and a cable pitch L_p=0.13 m) with a length of 1.3 m (=10L_p) is clamped over a length of 1.1 m (=8.5L_p) between two pressure bars. A transverse pressure on the cable of 15 MPa maximum can be applied by means of 30 bolts. The R_c-value can therefore be easily varied along the cable length. The strands in the two end sections of the cable, with a length of 10 cm, are in loose contact but can be soldered together to simulate the influence of cable-to-cable joints on the BICCs.

At uniform pressure, the distribution of the contact resistance over the cable length can be, approximately, represented by five regions with contact resistances $R_{c,1}$ to $R_{c,5}$ (see Fig. 1). The central part with a length of 1.1 m covers the section which is pressurised at about 10-15 MPa. In this section the contact resistance ($R_{c,3}$) is estimated to be about 20 μΩ, based on loss measurements as a function of the pressure on a similar cable with the same strand coating [4]. The contact resistances in the cable ends are estimated to be about 1 μΩ ($R_{c,1}$ and $R_{c,5}$ if soldered) and >>100 μΩ ($R_{c,2}$ and $R_{c,4}$, and $R_{c,1}$ and $R_{c,5}$ if not soldered).

Manuscript received August 26, 1996.

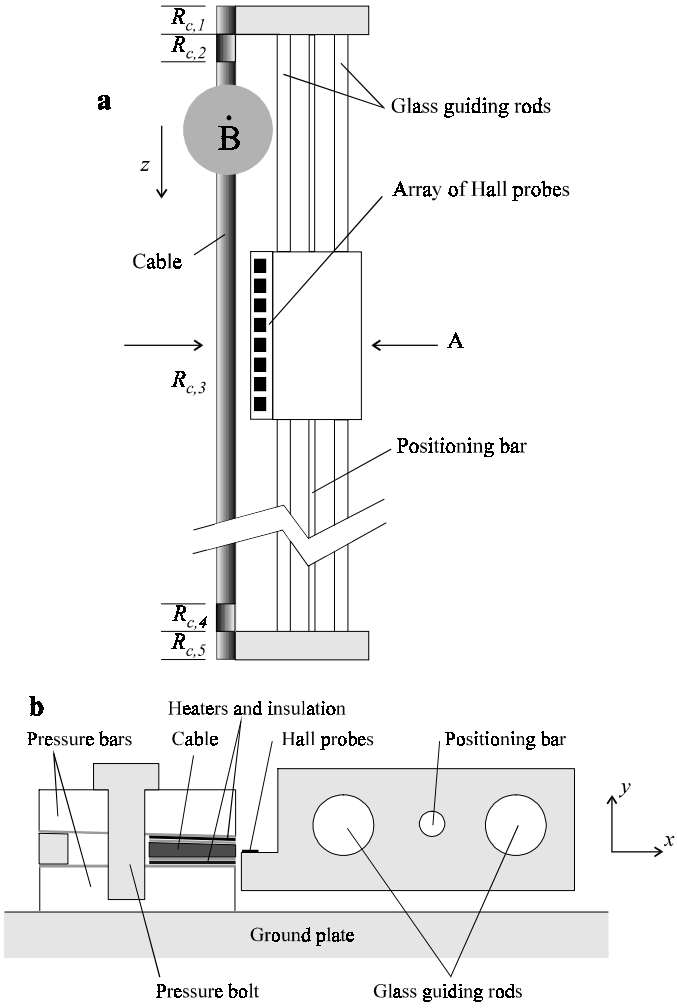

Fig. 1. **a.** Front view of the set-up, **b.** Cross-section of the set-up at A.

A stainless-steel heater, electrically insulated from the pressure bar and the cable, is fixed on the large faces of the cable in order to drive the cable into the normal state. Small heaters are locally placed on several strands to be able to drive the currents in these strands above their critical value.

The field in the *y*-direction is determined by an array of eight Hall probes, each having an active area of about 1 mm^2. The centre of the probes is located at a distance of 2 mm from the narrow side of the cable. The probes are fixed on a small sled which can move in the longitudinal (=*z*-) direction over two glass guiding rods. The *z*-position of the sled can be adjusted from outside the cryostat by means of a positioning bar with an accuracy better than 0.2 mm.

Two strands of the cable are connected to a current supply in order to calibrate the Hall probes.

A transverse field of 1.4 T maximum can be applied by means of a set of superconducting coils, located on both sides of the cable. The centre of the magnet is located at $z=0$. The cable lengths on either side of the magnet centre are 19 cm ($=1.4L_p=l_{cab,1}$) and 111 cm ($=8.5L_p=l_{cab,2}$). The $\dot{B}_\perp(z)$-distribution caused by the set of coils when ramped from 0 to 1.4 T in 10 s is shown in Fig. 2. In the following the $\dot{B}_\perp$-value refers to the maximum field-sweep rate at $z=0$.

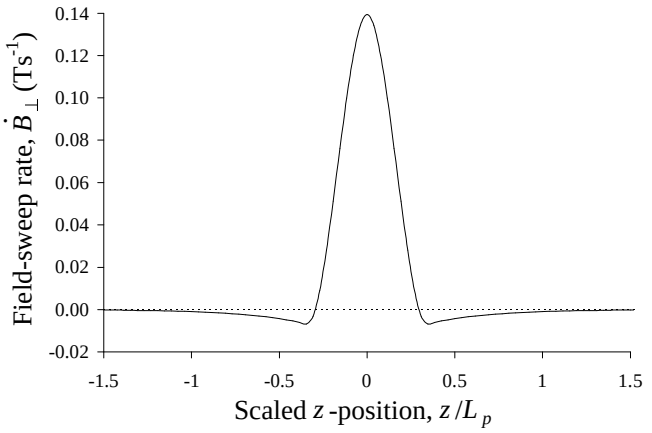

Fig. 2. The applied field change $\dot{B}_\perp$ at the centre of the cable along the cable length, for a field sweep of the set of coils from 0 to 1.4 T in 10 s.

III. Results

The magnitude of the steady-state BICCs for the given $\dot{B}_\perp$- and R_c-distributions is calculated by means of the network model. The simulations are performed for a cable with the same geometry and number of strands as the measured cable. The total field B_{bi} caused by the BICCs is calculated by superposition of the fields caused by the BICCs in each strand. Calculations of the characteristic time τ_{bi} and the propagation velocity $v_{bi}=d\tau_{bi}/dz$ for this cable with its specific $\dot{B}_\perp$- and R_c-variations are not performed. First estimates of τ_{bi} and v_{bi} are made using formulas for a single $\dot{B}_\perp$ step.

Field B_{bi} and τ_{bi} are determined as a function of the *z*-position in the range $0.5L_p<z<7.5L_p$. Measurements are performed for three different R_c-distributions along the cable length (see Fig. 1):

I: a cable with unsoldered ends, i.e. $R_{c,1}$, $R_{c,2}$, $R_{c,4}$ and $R_{c,5}$ are much larger than $R_{c,3}$,
II: a cable with one soldered end, i.e. $R_{c,1}$ is about 1 μΩ, whereas the other R_c-values remain unchanged,
III: a cable with two soldered ends, i.e. $R_{c,1}$ and $R_{c,5}$ are about 1 μΩ, whereas the other R_c-values remain unchanged.

The field measured by the Hall probes consists of:
- the stray field of the magnet B_{stray},
- the fields B_{is} and B_{if} produced by the Interstrand and the Interfilament Coupling Currents,
- the field B_{bi} produced by the BICCs, and
- the field B_m due to the filament magnetisation caused by B_{stray}, B_{if}, B_{is} and B_{bi}.

Field B_{bi} can be quite easily distinguished from the other field contributions, because:
- the fields B_{is} and B_{if} are negligible compared to B_{bi},
- the stray field and the magnetisation due to the stray field can be determined using a very small field-sweep rate,
- the magnetisation due to the coupling currents is relatively small compared to B_{bi} itself.

Characteristic fields B_{bi} as measured with the Hall probes are shown in Fig. 3 at a field sweep from 0 to 1.4 T with 0.019 Ts^{-1} for case II (a cable with one soldered end).

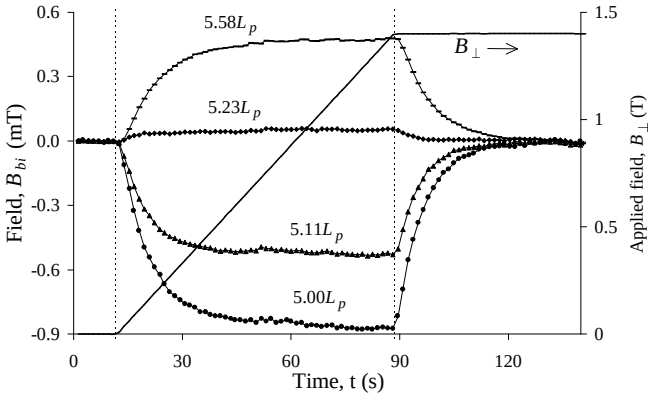

Fig. 3. Field $\boldsymbol{B}_{bi}$ measured simultaneously by four Hall probes during and after a field sweep from 0 to 1.4 T (see the straight line) with $\dot{B}_\perp = 0.019$ Ts^{-1}. The labels indicate the z-positions of the Hall probes. The dotted lines show the start and the end of the field sweep.

The figure shows clearly that the fields B_{bi} approach their steady-state values with $\tau_{bi} \approx 10$ s. Measurements at various field-sweep rates prove that the steady-state fields (and hence the BICCs) are proportional to $\dot{B}_\perp$ whereas the characteristic time is independent of $\dot{B}_\perp$. Both results agree with the calculations.

The steady-state field B_{bi} is measured for $0.5L_p < z < 7.5L_p$ and depicted in Fig. 4 for case I with $\dot{B}_\perp = 0.068$ Ts^{-1}. The continuous line corresponds to the calculated field using the network model with a constant resistance $R_{c,3}$=100 μΩ, infinite resistances $R_{c,1}$, $R_{c,2}$, $R_{c,4}$, $R_{c,5}$ and a very small ρ_{bi}, so that the BICCs decay linearly towards the ends of the cable.

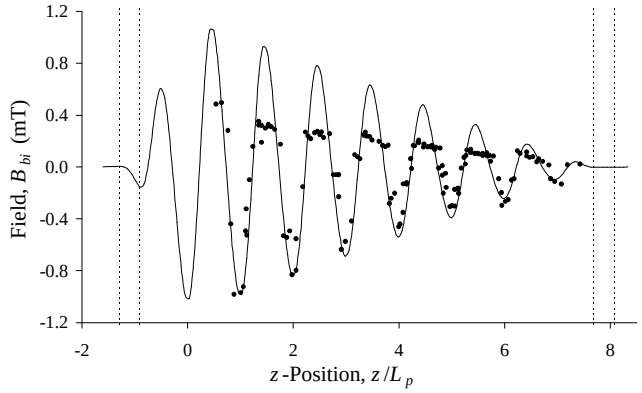

Fig. 4. Field $\boldsymbol{B}_{bi}$ as a function of z for case I with $\dot{B}_\perp = 0.068$ Ts^{-1}. The dotted lines show the boundaries between the sections with different R_c. The continuous line corresponds to the calculated field using the network model.

The value for $R_{c,3}$ is large compared to the expected value of 20 μΩ, which could be caused by an overall decrease in the pressure on the cable due to different shrinkage of the pressure bolts, the cable, the heaters and the insulation (see Fig. 1b) during cool-down. An increase in R_c near $z=0$ also results in significantly smaller BICCs even if R_c in the rest of the cable is much smaller.

The shape of the curve (with period L_p) does not depend on $R_{c,3}$ and corresponds very well with the measured one.

Both the calculated curve and the measured points have the same phase and decay linearly to 0 at the end of the cable, which proves that also the BICCs decay linearly to 0. The flattening in the maxima of the measured field is probably caused by a few strands that carry slightly smaller BICCs than expected, due to stronger oxidation of the surfaces of these strands (and hence a larger R_c) or due to local variations in R_c, especially at $z<0$.

Fig. 5 shows the characteristic time $\tau_{bi}(z)$ of the BICCs as a function of z, determined from the decay of the field after a ramp from 1.4 T to 0 with $\dot{B}_\perp = -0.068$ Ts^{-1}. Time $\tau_{bi}(z)$ is calculated for those positions which correspond to the maxima and minima in the field B_{bi} of Fig. 4.

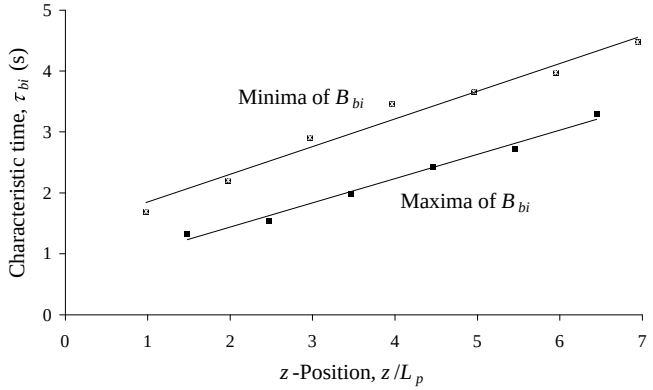

Fig. 5. The characteristic time of the BICCs as a function of z measured after a field sweep from 1.4 T to 0 with $\dot{B}_\perp = -0.068$ Ts^{-1}. The τ_{bi}-values are determined at those positions which correspond to the maxima and minima in B_{bi} of Fig. 4. The lines are linear fits.

The curves show that the BICCs diffuse into the cable with a constant propagation velocity v_{bi}. The average time constant is slightly larger in the minima than in the maxima. This difference is probably related to the flattening in the curves of Fig. 4, since a flattening implies a larger series resistance in the BICC loop and hence a decrease of the characteristic time.

It is interesting to investigate whether the formulas derived using the network model, which are valid in the case of a single $\dot{B}_\perp$-step, can also be applied to estimate the average characteristic time $\tau_{bi,av}$ and velocity $v_{bi,av}$ for this cable exposed to the $\dot{B}_\perp$-distribution as shown in Fig. 2.

- $\tau_{bi,av} = 6.2 \cdot 10^{-8} l_{cab,1} l_{cab,2} N_s^2/(LR_c) = 0.3$ s [4] (taking $N_s = 26$, $R_c = 100$ μΩ, $l_{cab,1} = 0.09$ m, $l_{cab,2} = 1.01$ m, $L_p = 0.13$ m), which is about a factor 7 smaller than the measured one (see Fig. 5 at about $z = 3L$).
- $v_{bi,av} = 1.7 \cdot 10^7 LR_c/(N_s^2 l_{cab,2}) = 0.3$ ms^{-1}, for $z \geq 0$ [4], which corresponds exactly to the experimentally obtained $v_{bi,av}$ as deduced from the average slope of Fig. 5.

In order to investigate the influence of sections with small R_c on the characteristics of BICCs, the R_c-distribution along the cable length is changed by soldering the ends of the cable with SnAg. Field B_{bi} is depicted in Fig. 6a/b for cases II and III respectively.

The magnitude of B_{bi} increases strongly due to the local solderings, whereas the phase remains constant, in good agreement with the result from the network model.

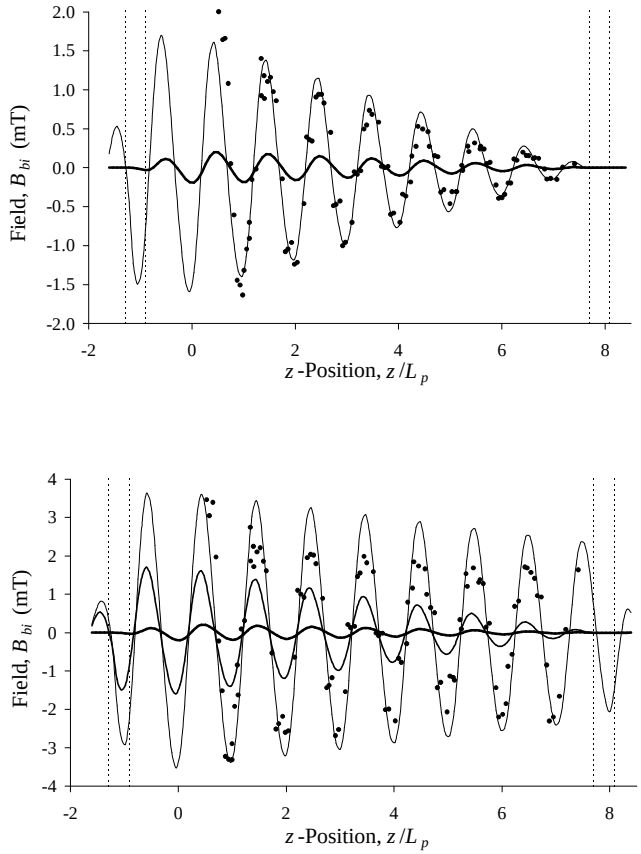

Fig. 6. Field $\boldsymbol{B}_{bi}$ as a function of z with $\dot{B}_\perp = 0.016$ Ts^{-1}. The dotted lines show the boundaries between the sections with different R_c. The continuous lines correspond to the calculated field using the network model. **a.** case II (the bold line shows the fitted curve of case I scaled to $\dot{B}_\perp = 0.016$ Ts^{-1}). **b.** case III (the bold lines correspond to cases I and II scaled to $\dot{B}_\perp = 0.016$ Ts^{-1}).

The calculated field, using the network model, can be fitted to the measurements by assuming a very small ρ_{bi} and taking:

– $R_{c,1}=1.2$ μΩ and $R_{c,3}=100$ μΩ (case II),
– $R_{c,1}=1.2$ μΩ, $R_{c,3}=100$ μΩ and $R_{c,5}=4$ μΩ (case III).

It can therefore be concluded that a soldered joint (with length l_{joint} and $R_c=R_{c,joint}$) in a coil influences the magnitude of the BICCs, especially if $l_{joint}/R_{c,joint}$ is larger than $l_{diff}/R_{c,cab}$, with $R_{c,cab}$ the average R_c of the cable and l_{diff} the length between the joint and the $\dot{B}_\perp$-variation. Note that if the joint itself is placed in a varying field, then additional BICCs will be induced caused by the R_c-step at the boundary between the joint and the rest of the cable [4].

The characteristic times of cases II and III increase, compared to case I, by about a factor 4 and 10 respectively. Although no calculations are performed, the increase can be well understood by considering that the average loop length of the BICCs becomes larger while the series resistance in the loops (i.e., in first approximation, the equivalent resistance of the parallel R_c's) becomes smaller. The propagation velocity of the BICCs remains constant for $0.5L<z<7.5L_p$. Calculations show a similar result, where the propagation velocity at position z is mainly determined by the *local* R_c at position z.

The large characteristic times of up to 30 s (for case III) show that very large $\tau_{bi,av}$-values of the order of 10^5 s may occur in magnets (since $\tau_{bi,av}$ is proportional to $l_{cab,1}l_{cab,2}$), with a cable length much larger than 1 m, if the BICCs diffuse to the ends of the cable. The observation of characteristic times of about 100-1000 s in several LHC dipole model magnets [4],[8] implies, therefore, that the BICCs decay over much smaller lengths than the actual length of the cable in the magnet.

V. Conclusion

The existence of BICCs is experimentally demonstrated in a 1.3 m long Rutherford-type cable exposed to a small local field change. The observed characteristics of BICCs:

– the *linear* decrease of the BICCs towards the cable ends,
– the oscillation of B_{bi} with a *period* equal to L_p, and
– the presence of a characteristic time which increases almost *linearly* along the cable,

agree qualitatively well with the calculations using the network model.

Quantitative differences of up to a factor of about 5 are probably caused by the unknown variations in R_c along the cable. The fact that the magnitude of BICCs in a single cable is already hard to assess shows that the BICCs in an entire coil will be even more complicated to calculate, especially if the spatial R_c-distribution is not well-known.

The magnitude of the BICCs can be reduced by increasing the contact resistances between the strands, for example by insertion of a resistive barrier in-between the two layers of a Rutherford-type cable or by applying a coating on the strands. However, local decreases in R_c (e.g. in the cable-to-cable connections in a coil) could significantly increase the magnitude and the characteristic time of the BICCs *caused by a* $\dot{B}_\perp$ *non-uniformity*. This implies that even in cables having a large R_c, BICCs will anyhow be present once the cable is locally soldered (even if the soldered parts are located in a low-field region).

References

[1] S. Takács, "Coupling losses in cables in spatially changing ac fields", *Cryogenics*, vol. 22, pp. 661-665, 1994.

[2] A.A. Akhmetov, A. Devred, and T. Ogitsu, "Periodicity of crossover currents in a Rutherford-type cable subjected to a time-dependent magnetic field", *J. Appl. Phys.*, vol. 75 (6), pp. 3176-3183, 1994.

[3] A.P. Verweij, and H.H.J. ten Kate, "Super Coupling Currents in Rutherford type of cables due to longitudinal non-homogeneities of dB/dt", *IEEE Trans. On Appl. SC*, vol. 4, pp. 404-407, 1995.

[4] A.P. Verweij, *Electrodynamics of Superconducting Cables in Accelerator Magnets*, PhD thesis University of Twente, The Netherlands, 1995.

[5] Krempasky, C. Schmidt, "Influence of a longitudinal variation of dB/dt on the magnetic field distribution of accelerator magnets", *Appl. Phys. Lett.*, vol. 66(12), pp. 1545-1547, 1995.

[6] A.P. Verweij, "Modelling Boundary-Induced Coupling Currents in Rutherford-type cables", unpublished (paper LMB-13 at ASC'96, Pittsburgh, USA).

[7] A.K. Ghosh, K.E. Robins, and W.B. Sampson, "The ramp rate dependence of the sextupole field in superconducting dipoles", *IEEE Trans. on Magn.*, vol. 30, pp. 1718-1721 (1994).

[8] L. Bottura, Z. Ang, and L. Walckiers, "Experimental evidence of Boundary-Induced Coupling Currents in LHC prototypes", unpublished (paper LQB-4 at ASC'96, Pittsburgh, USA).